2016 IEEE First Conference on Connected Health: Applications, Systems and Engineering Technologies

Sensing From the Bottom: Smart Insole Enabled Patient Handling Activity Recognition Through Manifold Learning

Feng Lin*, Chen Song*, Xiaowei Xu*, Lora Cavuoto†, Wenyao Xu*
*Department of Computer Science and Engineering
†Department of Industrial and Systems Engineering
University at Buffalo (SUNY), Buffalo, New York 14260
Email: {flin28, csong5, xiaoweix, loracavu, wenyaoxu}@buffalo.edu

***Abstract*—The risk of overexertion injury caused by patient handling and movement activities causes chronic pain and severe social issues among the nursing force. The accurate recognition of patient handling activities (PHA) is the first step to reduce injury risk for caregivers. In this paper, we propose a novel solution comprising a smart footwear device and an action manifold learning framework to address the challenge. The wearable device, called Smart Insole, is equipped with a rich set of sensors and can provide an unobtrusive approach to obtain and characterize the action information of patient handling activities. Our proposed action manifold learning (AML) framework extracts the intrinsic signature structure by projecting raw pressure data from a high-dimensional input space to a low-dimensional manifold space. We performed a pilot study with eight subjects including eight common activities in a nursing room. The experimental results show the overall classification accuracy achieves 86.6%. Meanwhile, the qualitative profile and load level can also be classified with accuracies of 98.9% and 88.3%, respectively.**

***Keywords*-Patient handling activity; action manifold learning; plantar pressure; Smart Insole; wearable health.**

I. Introduction

All healthcare workers, especially nurse and nursing workers, face a wide range of hazards on the job, such as musculoskeletal disorders related to ergonomic hazards [1]. These disorders are associated with excessive back and shoulder loading due to manual patient handling, applying excessive forces during pushing and/or pulling of objects, required use of awkward postures during patient care, and working long hours and shiftwork [2].

The high injury rate of nurses is because there is no effective approach to monitor the chronic injury development and detect acute overexertion, therefore, not much proactive prevention can be done to protect the nurses' health. Currently, assessment of working exposure by observation is a common practice in ergonomics [3]. However, several aspects of limitations cause visual inspection fail to provide accurate quantification of physical exposures, such as the observation-based assessment results are subjective from observers and failing to integrate multi-faceted traits [4], in addition, the observation duration and the number of workers being inspected are both restricted [5]. As a result, automatic patient handling and movement activity recognition is of importance and the first step for prevent injury risk for caregivers.

The development of advanced technology brings the possibility of more complete assessment and monitoring in nursing workspace. The widely used approach is the computer vision systems for monitoring the user activity and behavior in nursing rooms [6]. However, computer vision system requires costly installation and maintenance effort. The post-processing of data involves complex video and image algorithms, making the system at a high price. Furthermore, immobility, occlusion, and varying illuminations raise technical challenges in recognizing objects in the video [7]. Privacy invasion is also a concern from video monitoring. Wearable sensing system, such as a miniaturized inertial motion unit (IMU), is a promising approach to caregiver monitoring due to the nature of the handling and movement tasks performed. In order to monitor complex patient handling activities, multiple IMU sensors attached on different body locations are often needed [8], which causes hassle for long-term use and normal patient handling work in the nursing room [9].

Compared to daily life activity (DLA) recognition, patient handling activity (PHA) recognition is a challenging and substantially unexplored topic. PHA is a complex process and usually involves an interactive procedure between healthcare workers and loads (e.g., patients, medical instruments). Safe patient handling activities follow standardized procedure to prevent injury to both patients and caregivers, which are constrained by regulated operation, physical body kinematics, and the temporal constrains posed by the activities being performed. Given these constraints, PHA primitive, also called "action signature", can be extracted and represented in a low-dimensional manifold space embedded in a high-dimensional input space. Furthermore, these manifolds capture the intrinsic geometry of activities and act as trajectories to characterize different PHAs. Action signatures are usually nonlinear and even twisted, so dimension reduction by linear model such as principal component analysis (PCA) fail to discover the underlying geometric structures.

In this work, we propose a novel solution to overcome the

978-1-5090-0943-5/16 $25.00 © 2016 IEEE
DOI 10.1109/CHASE.2016.22

aforementioned obstacles in PHA recognition, which comprise a Smart Insole and an action manifold learning (AML) framework. Smart Insole is a novel footwear device which utilizes an advanced electronic textile (eTextile) fabric sensor technique providing accurate plantar pressure measurement in both ambulatory and static status. Smart Insole looks and feels like a normal insole without any extra cable, antenna, or adhesive equipment. It is also thin, light weighted and easy to use, enabling unobtrusive monitoring of human activities.

Action manifold learning is able to project high-dimensional data into a low-dimensional manifold space. By capturing the fundamental signature of action, only the intrinsic primitive structure are preserved in this transform, whereas unrelated motion artifacts and noise are neglected. Therefore, AML not only performs dimension reduction but also suppress motion artifacts and noise, which efficiently solves the variation problem in both inter-class and intra-class activities. In this proposed framework, raw pressure data are used rather than extracted statistical features, which is more robust because raw data utterly capture the direct pressure variation imposed by the activities.

We conduct a quantitative evaluation in a controlled environment and a real-life longitudinal study for AML framework. The experimental results show our method succeeds in qualitative profile recognition, PHA recognition, and load estimation with the overall classification accuracy of 98.9%, 86.6%, and 88.3%, respectively.

II. Background and Preliminaries

A. Related Work

Manifold learning has been widely applied in activity recognition by virtue of the capability of capturing the low-dimensional nonlinear manifolds embedded in the high-dimensional input space. Huang *et al.* [10] used a dense pressure sensitive bedsheet to produce pressure map, and the pressure images are processed by locally linear embedding (LLE) and ISOMAP for on bed rehabilitation exercises. Huang *et al.* [11] employed manifold learning for Electrocardiograph (ECG) signals dimension reduction and purification. Its applications to human action recognition can be classified into two categories. The first is video-based. For example, Wang *et al.* [12] learned the intrinsic object structure for robust visual tracking by using ISOMAP algorithm. Blackburn *et al.* [13] recognized human motion by using ISOMAP and dynamic time warping. The second is inertial motion unit (IMU) based. For example, Zhang *et al.* [14] used LLE to capture the intrinsic structure of IMU data and build nonlinear manifolds for daily life activities. Valtazanos *et al.* [15] applied translation manifold to inertial senor data for posture and position tracking.

B. Smart Insole

In the preliminary work, our team has developed the Smart Insole system [16] [17] [18] [19], we will briefly introduce the system design and functions in this section.

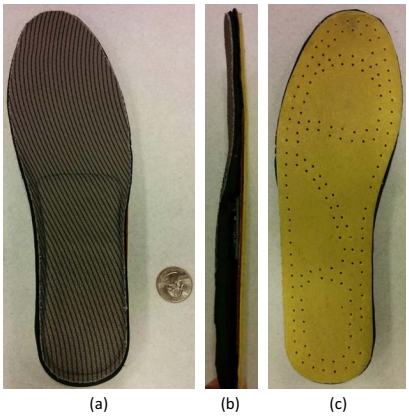

Figure 1. The human ergonomic prototype of Smart Insole: (a) Front view; (b) Lateral view; (c) Back view.

Smart Insole is a novel wearable device for activity monitoring, which is able to accurately capture the plantar pressure variation caused by the ongoing activity. The plantar pressure is obtained by the low-cost pressure sensor array, which is based on an advanced conductive eTextile fabric sensor technique [20] [21]. The eTextile pressure sensor array is used to obtain the high-solution pressure map from feet, which can be efficiently integrated in Smart Insole. The sensor array is coated with a piezoelectric polymer, and the initial resistor between the top-bottom surfaces is high. When extra force is applied on surface of the polymer, the inner fibers will be squeezed together and the throughout resistor becomes smaller. As a result, the output voltage level will be high. Each pressure sensor is with the size of $15\text{mm} \times 15\text{mm}$. With 48 sensors in total, more than 80% of the plantar area is covered.

We design a printed circuit board (PCB) to integrate the MCU and Bluetooth module, the inertial motion unit (IMU) module, the micro-USB connector, the power switch, and the battery conditioning circuits together. The MCU and Bluetooth are implemented by a single device CC2541 from Texas Instruments. CC2541 also contains an 8-channel, 12-bit, and 0-3.3 volt analogue-to-digital converter (ADC) module, which can provide up to 100 samples per second (Hz). The integrated IMU chip contains a 12-bit accelerometer, a 16-bit gyroscope, and a magnetometer, which is able to capture precise motion information with 9 degrees of freedom motion sensing. The human ergonomic prototype of Smart Insole is shown in Fig. 1 with front view, lateral view, and back view.

III. Action Manifold Learning (AML) Framework on Underfoot Pressure Maps

In this section, we will present the AML framework on underfoot pressure maps for patient handling activity (PHA) recognition. The diagram of the overall system design

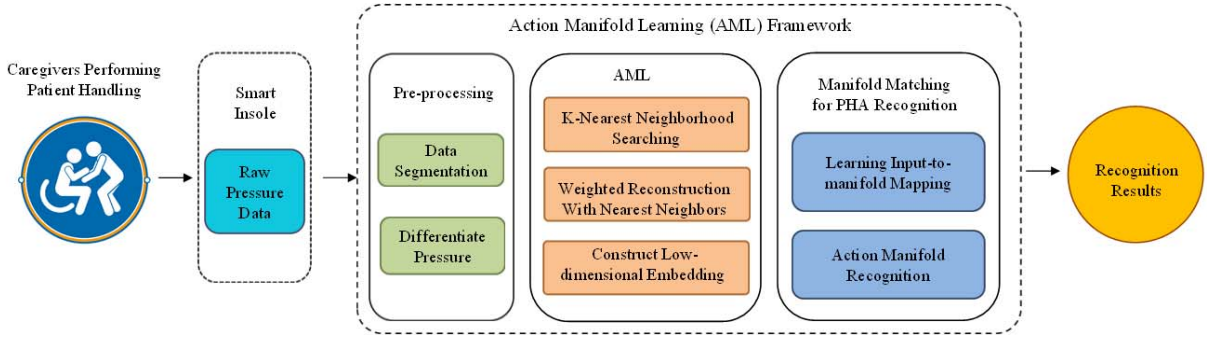

Figure 2. The diagram of the overall system design including Smart Insole and the AML framework for PHA recognition.

including Smart Insole and the AML framework for PHA recognition is shown in Fig. 2. Caregivers activities and recognition results are the input and output of the system.

A. Action Manifold Learning Framework

The processing flow of the action manifolding learning framework-based PHA recognition is shown in Fig. 3. The AML framework consists training stage and testing stage. In training stage, the high-dimensional pressure data after pre-processing are mapped into a low-dimensional manifold space by constructing action manifold to find the action signature for each PHA. Patient handling and movement activities [22] [23] are the tasks involving transfer of a load or patient. Safe PHAs follow standardized procedure in order to prevent the risk to the caregivers' lumbar spine and injury to the patient, so the low-dimensional action signature in pressure distribution can be extracted in manifold space. In testing stage, the unlabeled actions are mapped into the low-dimensional manifold space by the input-to-manifold projection mapping function and matched to the closest training action manifold.

B. Pre-processing

The pre-processing of raw pressure maps is required so that the pressure maps can be standardized in such a way to enable successful recognition. First, only the useful primitive action is contained in each set of data samples, unrelated actions or vibrations are eliminated. Second, we obtain the differential of the raw pressure data. The differential of pressure $x_i\left(t\right)$ is calculated as:

$$\mathrm{p_i}\left(t\right)=\frac{\mathrm{dx_i}\left(t\right)}{\mathrm{d}t},1\leq i\leq D, \tag{1}$$

where i is the index of pressure sensor, and D is the number of pressure sensor as well as the dimension of the pressure data in input space (in this case $D=48$). The reason we adopt differential is because it is robust against the spurious signals, different offset of the insoles, and different weights of subjects.

C. Action Manifold Learning

In action manifold learning, we adopt LLE framework [24] to capture the intrinsic low-dimensional structures of the PHA. The reason LLE is a good candidate for action manifold learning is that LLE makes few assumptions about the activities [25] and runs fast by avoiding the need to solve large dynamic programming problem [26]. After the computation, similar pressure distribution will be clustered within the low dimensional manifold.

Let $\mathbf{P}=\left\{\mathbf{p}_i\in R^D,i=1,\cdots,N\right\}$ be the differential of raw pressure data from PHA signal with sample length of N, where $\mathbf{p}_i$ represents the ith sample of input data and acts as a single point in R^D. Action manifold learning maps D-dimensional $\mathbf{P}$ into d-dimensional manifold space ($d\ll D$). The steps of LLE procedure is described in the following.

1) K-Nearest Neighborhood Searching: The first step is to find the K nearest neighbors (kNN) for each point $\mathbf{p}_i,i=1,\cdots,N$ in the input space. In the searching process, we use Euclidean distance to measure the similarity between pressure distributions of each sample. The value of K is determined empirically.

2) Weighted Reconstruction With Nearest Neighbors: The second step is to reconstruct a sample pressure distribution using its nearest neighbors assuming that each point and its nearest neighbors lie on a locally linear patch of the underlying manifold. In practice, an exact reconstruction may not be found, so the reconstruction weights are determined by minimizing the global reconstruction error. The reconstruction error e for a single point can be formulated as:

$$e_i=\left\|\mathbf{p}_i-\sum_{j=1}^{K}w_{ij}\mathbf{p}_{ij}\right\|^2, \tag{2}$$

The global error E can be represented by accumulating N errors together:

$$E=\sum_{i=1}^{N}\left\|\mathbf{p}_i-\sum_{j=1}^{K}w_{ij}\mathbf{p}_{ij}\right\|^2, \tag{3}$$

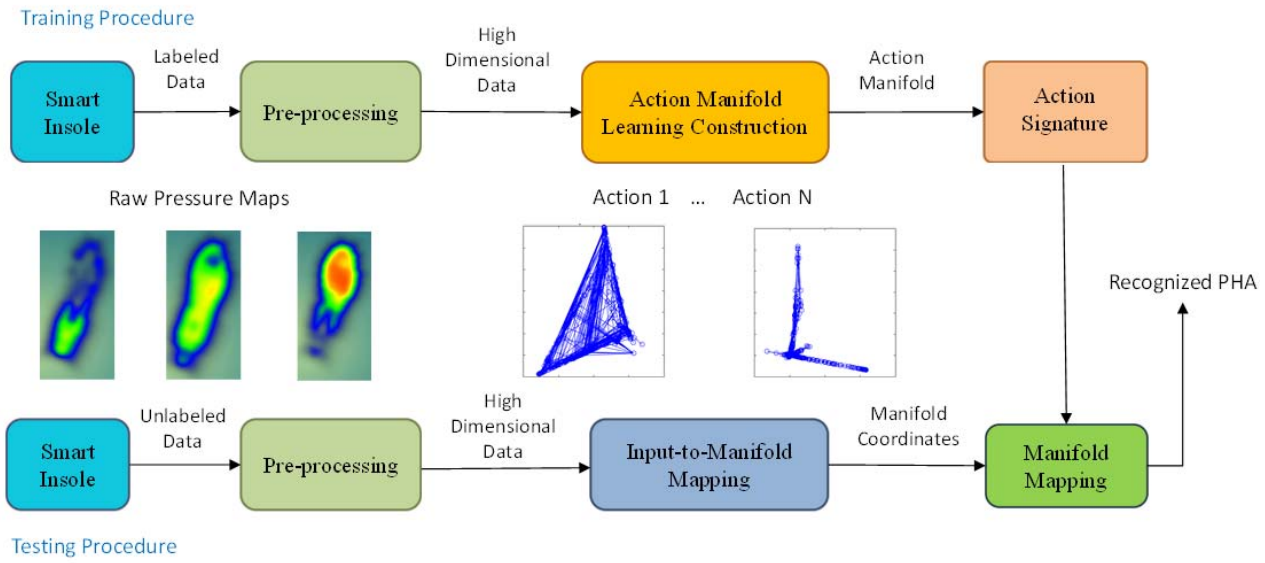

Figure 3. Processing flow of the action manifolding learning-based PHA recognition.

where w_{ij} denotes the reconstruction weight for the point $\mathbf{p}_i$ and its neighbors $\mathbf{p}_{ij}$. Two constraints are imposed to the cost function (3) to ensure the solution is feasible: (1) $w_{ij} = 0$, if $\mathbf{p}_{ij}$ is not in the nearest neighbors list of $\mathbf{p}_i$; (2) $\sum_{j=1}^{K} w_{ij} = 1$, if $\mathbf{p}_{ij}$ is among $\mathbf{p}_i$'s K nearest neighbors. The solution to Eq. (3) can be found by solving a least square problem [24].

3) Construct Low-dimensional Embedding: The third step is to construct the corresponding embedding in a low-dimensional space. Based on the calculation results from the second step, the intrinsic geometrical structure of each local cluster is characterized by w_{ij}. We assume that the neighborhood relation in high dimensional space should be preserved in low dimensional manifold space. Based on this assumption, the manifold coordinates $\mathbf{y}_i$ can be computed by minimizing the embedding cost function as:

$$\min_{\mathbf{Y}} \quad \Phi(\mathbf{Y}) = \sum_{i=1}^{N} \left\| \mathbf{y}_i - \sum_{j=1}^{N} w_{ij} \mathbf{y}_{ij} \right\|^2, \tag{4}$$

where $\mathbf{y}_i$ and $\mathbf{y}_{ij}$ are the corresponding points of $\mathbf{p}_i$ and $\mathbf{p}_{ij}$ in manifold space, respectively. The cost function can also be written as:

$$\Phi(\mathbf{Y}) = \sum_{i=1}^{N} \sum_{j=1}^{N} \mathbf{M}_{ij} (\mathbf{y}_i \cdot \mathbf{y}_j), \tag{5}$$

involving inner products of the embedding vectors and the $N \times N$ matrix $\mathbf{M}$:

$$\mathbf{M}_{ij} = \delta_{ij} - w_{ij} - w_{ji} + \sum_{k=1}^{K} w_{ki} w_{kj}, \tag{6}$$

where δ_{ij} is 1 if $i = j$, otherwise 0.

All the manifold points $\mathbf{y}_i$ will be computed globally and simultaneously, and no local optima will affect the construction result. Note that the coordinate $\mathbf{y}_i$ can be translated by a constant displacement without affecting the cost $\Phi(\mathbf{Y})$. We require the coordinates to be centered on the origin as:

$$\sum_{i=1}^{N} \mathbf{y}_i = 0, \tag{7}$$

and the embedding points to have unit covariance as:

$$\frac{1}{N} \sum_{i=1}^{N} \mathbf{y}_i \mathbf{y}_i^T = \mathbf{I}, \tag{8}$$

where $\mathbf{I}$ is the $d \times d$ identity matrix. These two constraints make the problem well-posed, thus, the optimal embedding is found by computing the bottom $d+1$ eigenvectors of the matrix $\mathbf{M}$ and discarding the most bottom eigenvector to get the desired d manifold coordinates [26].

D. Manifold Matching for PHA Recognition

1) Learning Input-to-manifold Mapping: Once the training data have been mapped to its corresponding low dimensional space, we can evaluate the process using new test data against the training data. Since running AML for the entire dataset with training and testing data is computationally expensive, we only execute a portion of the AML algorithm by adopting a non-parametric mapping function [24]. Given a new test pressure distribution $\hat{\mathbf{p}}$, we wish to find its low-dimensional representation $\hat{\mathbf{y}}$. First, the weights w_j are computed from the K nearest neighbors of $\hat{\mathbf{p}}$ in the training

set $\mathbf{p}_i$ by solving the least squares problem:

$$\min_{w} \left\| \hat{\mathbf{p}} - \sum_{j=1}^{K} w_j \mathbf{p}_j \right\|, \tag{9}$$

with the constraint $\sum_{j=1}^{K} w_j = 1$. Since the corresponding low-dimensional coordinates of $\mathbf{p}_i$ are known during the training phase, we can reconstruct the embedded coordinates for $\hat{\mathbf{y}}$ using the same weights w_j as:

$$\hat{\mathbf{y}} = \sum_{j=1}^{K} w_j \mathbf{y}_j, \tag{10}$$

where $\mathbf{y}_j$ are the corresponding embedded coordinates of $\mathbf{p}_j$.

2) Action Manifold Recognition: The action manifold recognition is performed by comparing the trajectories of manifolds in the low-dimensional space. We observe that the data lengths of each actions usually are disparate and different subjects take different time to perform each activity, therefore, an appropriate distance metric that can handle data length misalignment is needed. In this work, we adopt the Hausdorff distance [27] for similarity measurement metric. The Hausdorff distance of a point to a manifold is equal to the shortest Euclidean distance to any point in the manifold, that is, the mean value of the minimum, expressed as:

$$s\left(M_1, M_2\right) = \frac{1}{T_{M_1}} \sum_{i=1}^{T_{M_1}} \min_{1 \le j \le T_{M_2}} \left\| M_1\left(i\right) - M_2\left(j\right) \right\|, \tag{11}$$

where M_1 and M_2 are two manifolds under comparison, T_{M_1} and T_{M_2} are the number of points in each manifold. Since the Hausdorff distance is directional, we take the summation to ensure the symmetry of the distance metric as:

$$dist\left(M_1, M_2\right) = s\left(M_1, M_2\right) + s\left(M_2, M_1\right). \tag{12}$$

Based on this distance metric, we can measure the similarity between unlabeled activities and known activities, and the testing activity is classified as the activity class which has the most similar manifold with the testing activity.

IV. Evaluation

A. Experimental Setup

We ran a series of experiments in a laboratory environment to evaluate the performance of our proposed action manifold learning framework for PHA recognition. The dataset was collected by our Smart Insole from eight subjects including seven male subjects and one female subject. The weights of all participants are from $58-85$ kg and heights from $160-185$ cm. Each subject performed seven different PHAs including: (a) *bend leg to lift an item from floor level*; (b) *stand while lifting patients leg*; (c) *stand while lifting patient from wheelchair*; (d) *stand while rolling patient*; (e) *walk normally*; (f) *walk while pushing wheelchair forward*; (g) *walk with both hands carrying a chair*. To be specific, in (b), the subject lifted a patient's leg and keeps for three seconds then slowly puts down the leg. Likewise, in (d), the subject rolled over a patient and also kept for three seconds then rolled back to the original position. In (g), the subject first lifted the wheelchair up then walked forward with two hands carrying the wheelchair. We also performed a *sitting* activity in this evaluation though it is not directly related to patient handling or movement. In addition, sitting is static such that it is infeasible to use AML framework to extract a consistent trajectory. However, successfully recognizing sitting activity can help to estimate the workload in a nursing environment by knowing how long a caregiver take a break as sitting. To distinguish sitting from other activities, simply applying a threshold to p_i before AML is enough because sitting is static leading to p_i to be close to 0. For simplicity of description in this paper, we include sitting as one of the PHAs. The real experimental scenes are shown in Fig. 4.

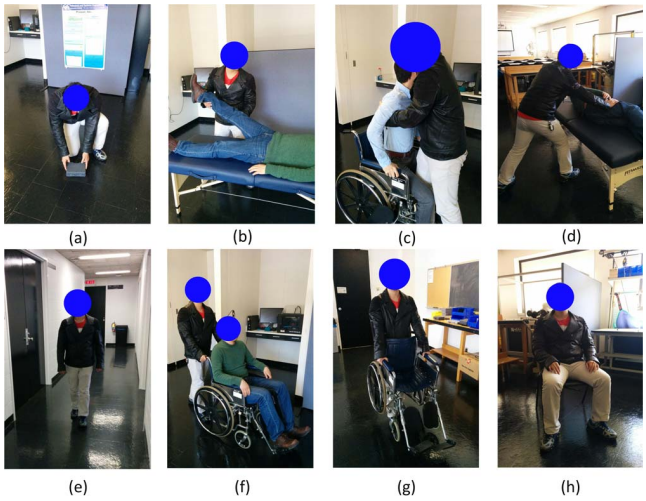

Figure 4. Eight different PHAs performed in experiments including: (a) Bend leg to lift an item from floor level; (b) Stand while lifting patients leg; (c) Stand while lifting patient from wheelchair; (d) Stand while rolling patient; (e) Walk normally; (f) Walk while pushing wheelchair forward; (g) Walk with both hands carrying a chair; (h) Sitting normally.

B. Action Signature Extraction

We visualize the 3-D raw pressure data from each PHA in Fig. 5. Since we observed that the curves with all 48 channels data from Smart Insole in one figure makes the pressure variation pattern too dense to be seen clearly, we pick up six out of 48 pressure points and show their waveforms for a better visualization. In Fig. 5, (a) *bend leg to lift an item from floor level* and (c) *stand while lifting patient from wheelchair* are "single action" based activities. (b) *stand while lifting patients leg* and (d) *stand while rolling patient* are "action-still-action" based activities, as can be observed

from Fig. 5 (b) (d) that a flat area indicating keeping still exists between two waves indicating actions. (e) *walk normally*, (f) *walk while pushing wheelchair forward*, and (g) *walk with both hands carrying a chair* are all walking related which show either periodic or pseudo-periodic pattern. The corresponding low-dimensional trajectories are shown in Fig. 6. Two "single action" activities (a) (c) are represented as the crossing lines in two direction. Two "action-still-action" activities (b) (d) are represented as the crossing lines in three direction. Because the pressure variation in keeping still status is small, the projected trajectory in manifold space as a consequence also has a small deviation, which results a shorter length comparing with the lines in other two directions. The walking activities in (e) (f) (g) evolve along a triangle shape in the manifold space. This is because these three activities are either periodic or pseudo-periodic causing the trajectories of different cycles overlap each other. Note that besides walking (g) also contains a *lifting chair* "single action", which results the trajectory exhibiting somewhat two crossing lines pattern.

C. Quantitative Evaluation in a Controlled Study

For this part, we evaluate the classification performance of our proposed framework by kNN. A leave-one-out cross-validation (LOOCV) is adopted to quantify the accuracy. In this quantitative evaluation, each subject is required to perform 10 trials on each activity. Therefore, total 640 trials are performed in our experiments.

1) Accuracy Evaluation: The quantitative evaluation performance is measured by classification accuracy. Given the large number of testing inquiries, the framework should offer the correct responses with high probability. The accuracy (ACC) is defined as:

$$ACC\ (\%) = \frac{TP + TN}{P + N} \times 100\%, \tag{13}$$

where TP represents the true positive, TN represents the true negative, P represents the positive, and N represents the negative. In injury risk estimation, qualitative profile recognition, PHA recognition, and load estimation are three key parameters [28]. PHA recognition is used for estimating injury probability for each PHA. Qualitative profile recognition and load estimation are used in estimating workload and load in performing PHA, respectively.

2) Qualitative Profile Recognition: Qualitative profile recognition is used to estimate the workload in a nursing environment. There are many solid facts that most of nurses suffered chronic occupational diseases. Based on the percentages of all-body activities (i.e., walk related), upper-body activities (i.e., standing related), and break (i.e., sitting) in a working period, we can infer the intensity level of the workload and the long-term fatigue level, so that the nurse can pay more attention in PHA to prevent the potential injuries. Here, all the aforementioned eight PHAs are categorized into three qualitative profiles as described in Table I, which facilitates the workload estimation. Both recall and precision achieve more than 97.9% as shown in Table I, which shows high performance of qualitative profile recognition. Note that the performance from qualitative profile recognition is better than the one with PHA recognition described in the following, which is because several confusing activities actually belong to the same qualitative profile such as *stand* or *walk*. In such case, these PHAs are treated as no difference in terms of qualitative profile. The *ACC* can reach 98.9%.

Table I
CONFUSION TABLE OF RECOGNITION ON THREE CATEGORIZED ACTIVITIES

	Stand (a, b, c, d)	**Walk (e, f, g)**	**Sit (h)**	**Total**	**Recall**
Stand (a, b, c, d)	315	5	0	320	98.4%
Walk (e, f, g)	2	238	0	240	99.2%
Sit (h)	0	0	80	80	100.0%
Total	317	243	80		
Precision	99.4%	97.9%	100.0%		

Table III
CATEGORIZATION OF PHA INTO LOAD LEVELS

	Load levels	**Activities description**
c	Heavy	Stand while rolling patient
d		Stand while lifting patient from wheelchair
g		Walk with both hands carrying a chair
a	Light	Bend leg to lift an item from floor level
b		Stand while lifting patients leg
f		Walk while pushing wheelchair forward
e	No	Sit normally
h		Walk normally

Table IV
CONFUSION TABLE OF RECOGNITION ON THREE CATEGORIZED LOAD LEVELS

	Heavy (c, d, g)	**Light (a, b, f)**	**No (e, h)**	**Total**	**Recall**
Heavy (c, d, g)	211	22	7	240	87.9%
Light (a, b, f)	23	209	8	240	87.1%
No (e, h)	6	9	145	160	90.6%
Total	240	240	160		
Precision	87.9%	87.1%	90.6%		

3) PHA Recognition: The goal of PHA recognition is to accurately classify each PHA defined in Fig. 4 . Table II shows the confusion table with respect to PHA classification using 48 pressure sensors. We notice the activity *walk with both hands carrying a chair* has the lowest recall rate 80.0%, which is often confused with *walk normally* and *walk while pushing wheelchair forward*. The reason of this is that all the three activities are performed in walking status, in which the pressure obtained from them all shows similar pseudo-periodic nature. Among them, *sit*

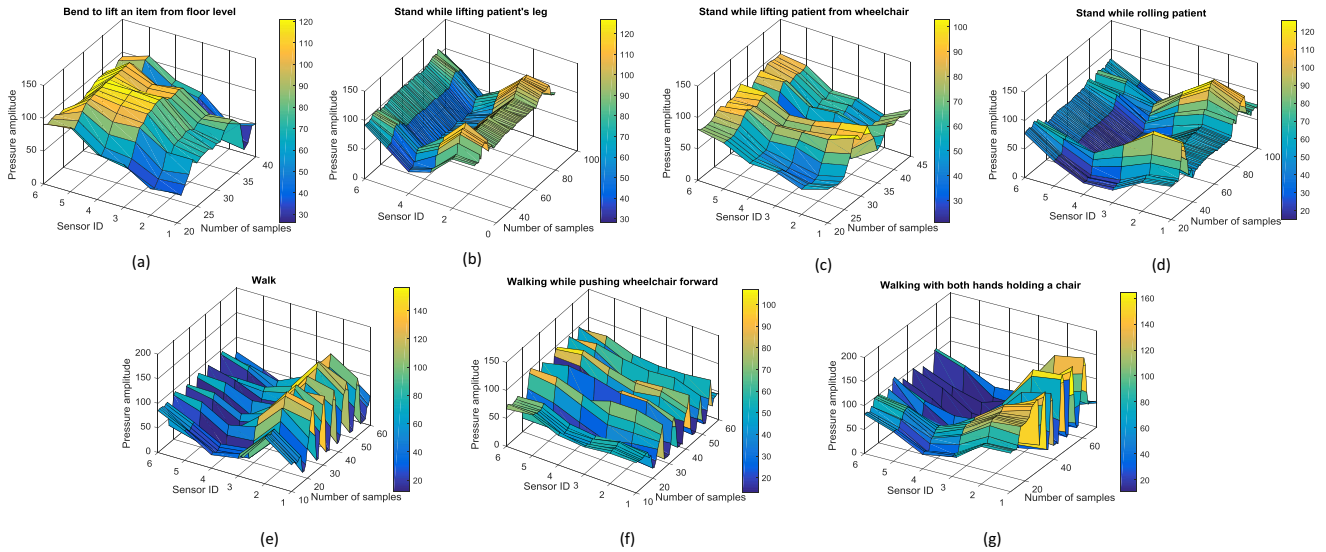

Figure 5. The 3-D visualization of pressure data from Smart Insole 2.0: (a) Bend leg to lift an item from floor level; (b) Stand while lifting patients leg; (c) Stand while lifting patient from wheelchair; (d) Stand while rolling patient; (e) Walk forward; (f) Walk while pushing wheelchair forward; (g) Walk with both hands carrying a chair.

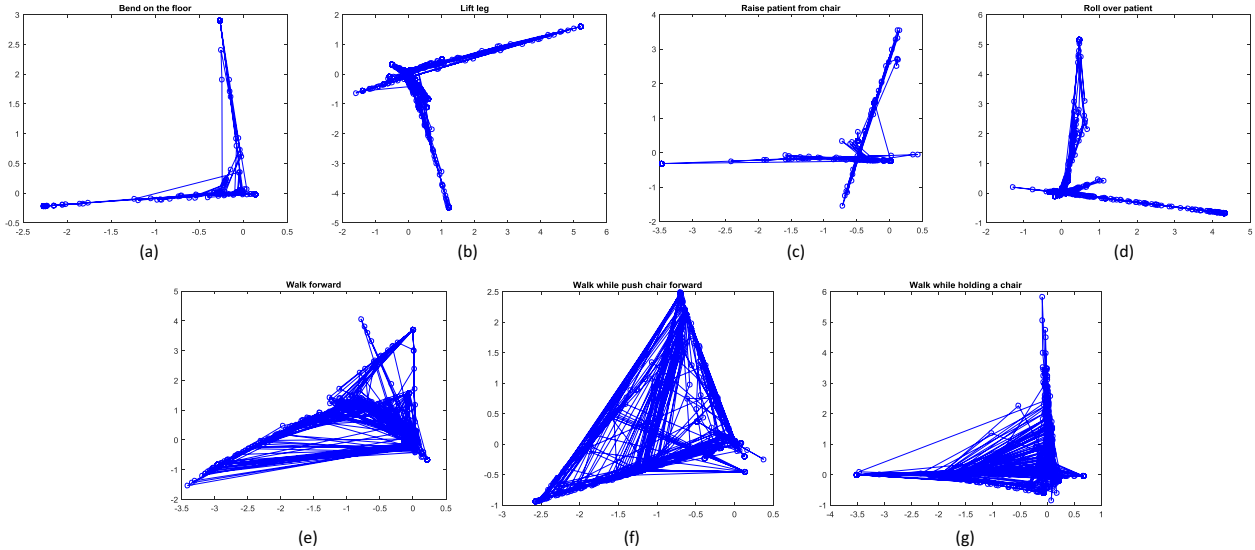

Figure 6. Visualization of PHA in manifold space: (a) Bend leg to lift an item from floor level; (b) Stand while lifting patients leg; (c) Stand while lifting patient from wheelchair; (d) Stand while rolling patient; (e) Walk forward; (f) Walk while pushing wheelchair forward; (g) Walk with both hands carrying a chair.

reaches 100% recall and 100% precision because of the minimal fluctuation it exposed that differentiates it from other activities. In terms of precision, *walk with both hands carrying a chair* also shows the lowest rate of 79.0% because the data from other activities show similarity to the data of *walk with both hands carrying a chair*, which results in the mis-classification. Overall, the *ACC* can reach 86.6%. This accuracy can be further improved by analyzing IMU data together with pressure data.

4) Load Estimation: The load estimation is to estimate the load imposed on caregivers when they perform certain PHA in order to prevent overexertion. The grouping criterion depends on the specific ongoing activity and how normal people feel when performing it. Note that we decide *bend leg to lift an item from floor level* as *light load* because that item the subject picked up indicates the specific weight

Table II
CONFUSION TABLE OF RECOGNITION ON 8 PHAS USING AML

	a	b	c	d	e	f	g	h	Total	Recall (Sensitivity)
a	69	2	7	0	0	0	2	0	80	86.3%
b	2	70	4	4	0	0	0	0	80	87.5%
c	7	2	67	1	0	0	3	0	80	83.8%
d	1	4	2	73	0	0	0	0	80	91.3%
e	0	0	0	0	65	9	6	0	80	81.3%
f	0	0	0	0	8	66	6	0	80	82.5%
g	1	0	1	0	7	7	64	0	80	80.0%
h	0	0	0	0	0	0	0	80	80	100.0%
Total	80	78	81	78	80	82	81	80		
Precision	86.3%	89.7%	82.7%	93.6%	81.3%	80.5%	79.0%	100%		
Specificity	98.0%	98.6%	97.5%	99.1%	97.3%	97.1%	97.0%	100%		

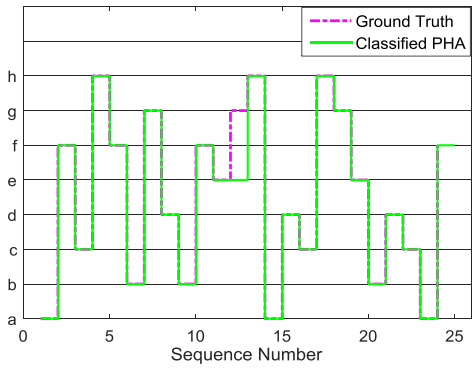

Figure 7. A set of eight PHAs performed randomly against ground truth.

of the object in our experiment. The load level category is summarized in Table III. Likewise, the confusion table with respect to load levels is shown in Table IV. *Light load* has the lowest recall of 87.1%, and *heavy load* has the similar recall of 87.9%. Since these two load level both involve forceful exertion, they easily confused with each other. The ACC can reach 88.3%.

D. Evaluation of a Longitudinal Pilot Study

To evaluate the proposed approach in an end-to-end test scenario, we carried out a pilot study in a real nursing room. The subject wearing Smart Insole performed a set of patient handling activities in a continuous manner. The activities include all actions in Fig. 4 in a random sequence. For the sake of repetition, each activity was performed more than once. We also videotaped the entire process as the label of ground truth. Fig. 7 shows the evaluation result, where the red dash line indicates the ground truth and the blue line indicates the actual classification outcome. We observed that only one out of 24 activities is mis-classified, which validates the effectiveness of the proposed AML framework in the real-life setup.

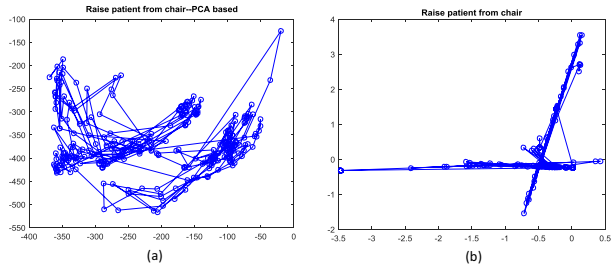

Figure 8. Visualization of two types of dimension reduction methods: (a) PCA (b) AML.

E. Comparison with PCA-based Dimension Reduction

Dimension reduction techniques are usually applied on large scale dataset to transform data into another domain to either make it more manageable or easy to analyze. PCA is a linear dimension reduction method that has widespread use. Fig. 8 illustrates the visualization trajectories of PCA and AML when performing the *stand while lifting patient from wheelchair* activity. We compare the performance of AML and PCA-based dimension reduction method [29] for PHA recognition in terms of accuracy, as shown in Table V. PCA has the accuracies of 84.3%, 71.5%, and 72.1% in the qualitative profile recognition, PHA recognition, and load estimation, respectively. Compared with PCA, AML is better suited to identify the underlying topological structure that is nonlinear in the high-dimensional space. Overall, AML outperforms PCA-based dimension reduction.

V. DISCUSSION

A. Impact of K in AML

The proper selection of K, the number of nearest neighbors defined in AML, has a big impact on the performance of AML. If K is too small, a continuous manifold may be divided into disjoint sub-manifolds. Actually, the LLE algorithm can only recover embeddings whose intrinsic dimensionality is less than K [24]. In contrast, a large K may violate the assumption of local linearity. Thus, we need to determine the optimal selection of K. We ran an

Table V
ACCURACY COMPARISON BETWEEN AML AND PCA

	AML	PCA
Qualitative Profile Recognition	98.9%	84.3%
PHA Recognition	86.6%	71.5%
Load Estimation	88.3%	72.1%

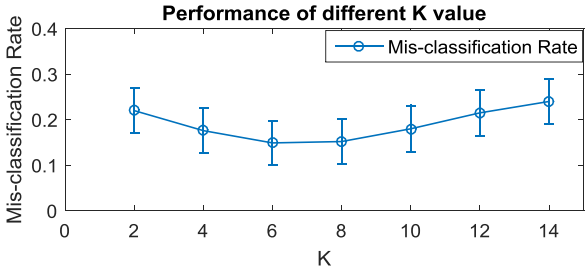

Figure 9. Performance impact of different K value for action manifold learning

experiment changing K from 2 to 14 step by 2 to find the optimal K in terms of lowest mis-classification error. The performance measured by the mis-classification rate is shown in Fig. 9, where the error bars represents the standard deviation. As seen from the figure, the lowest mis-classification rate is achieved at $K = 6$, and the performance of $K = 8$ is slightly worse. We conclude that using 6 nearest neighbors is optimal to construct the activity manifolds.

B. Distance Metrics

In AML framework, choosing appropriate distance metric is a critical step for similarity measurement, such as Euclidean distance (ED) [30], Hausdorff distance [27], and earth mover's distance (EMD) [31]. Among them, Euclidean distance provides 1-to-1 matching, both Hausdorff distance and EMD can provide matching under misalignment situation where Hausdorff distance can solve m-to-1 matching [32] and EMD can solve m-to-n matching. Compared with ED and EMD, Hausdorff distance is more suitable in our problem and is adopted in our proposed framework. Another potential distance metric is Kullback-Leibler divergence, which is a type of probability distance that measures the difference between two probability distributions. It is widely accepted to model ambiguity sets [33]. We will pursue using Kullback-Leibler divergence as the distance metric in our future work.

C. Generalization of AML

There are tunable parameters in the proposed AML framework (e.g. d, K), the choice of these parameters will make AML framework to achieve a good performance in practice. Safe patient handling activities follow standardized procedure to prevent injury, so the intrinsic dimension of PHA primitive d in the low-dimensional manifold space has small range of variation which is usually between 2 and 4. The intrinsic dimension can be found by training process of PHA and used in the classification phase of PHA. From the results presented in subsection V-A, the optimal choice of K is 6.

VI. CONCLUSION

Recognizing patient handling activities is the first step to estimate the physical injury risk for caregivers. We propose a solution comprising Smart Insole and an action manifold learning framework for accurately recognizing PHA. Smart Insole is capable of capturing the plantar pressure change information caused by the PHA. AML framework can find the intrinsic signature structure by performing nonlinear dimension reduction on raw pressure data from a high-dimensional input space to a low-dimensional manifold space. The experimental results showed that our framework can achieve 86.6% overall accuracy with eight different PHAs. Meanwhile, the qualitative profile and load level can also be classified with accuracies of 98.9% and 88.3%, respectively. Moreover, we also investigated the influence of the number of nearest neighbors (K) to the performance. In AML framework, $K = 6$ is the optimal selection to get the lowest mis-classification rate.

REFERENCES

[1] Public Health Service, "Centers for disease control and prevention worker health chartbook," US Department of Health and Human Services, Tech. Rep., 2000.

[2] T. Waters, J. Collins, T. Galinsky, and C. Caruso, "Niosh research efforts to prevent musculoskeletal disorders in the healthcare industry," *Orthopaedic Nursing*, vol. 25, no. 6, pp. 380–389, 2006.

[3] S. E. Mathiassen, P. Liv, and J. Wahlström, "Cost-efficient measurement strategies for posture observations based on video recordings," *Applied ergonomics*, vol. 44, no. 4, pp. 609–617, 2013.

[4] L. A. Cavuoto and M. A. Nussbaum, "Influences of obesity on job demands and worker capacity," *Current Obesity Reports*, vol. 3, no. 3, pp. 341–347, 2014.

[5] V. L. Paquet, L. Punnett, and B. Buchholz, "Validity of fixed-interval observations for postural assessment in construction work," *Applied ergonomics*, vol. 32, no. 3, pp. 215–224, 2001.

[6] A. Garg, B. Owen, and B. Carlson, "An ergonomic evaluation of nursing assistants' job in a nursing home," *Ergonomics*, vol. 35, no. 9, pp. 979–995, 1992.

[7] D. Chen, J. Yang, and H. D. Wactlar, "Towards automatic analysis of social interaction patterns in a nursing home environment from video," in *Proceedings of the 6th ACM SIGMM international workshop on Multimedia information retrieval*. ACM, 2004, pp. 283–290.

[8] Z. Zhang, W. C. Wong, and J. Wu, "Wearable sensors for 3d upper limb motion modeling and ubiquitous estimation," *Journal of Control Theory and Applications*, vol. 9, no. 1, pp. 10–17, 2011.

[9] B.-H. Yang, S. Rhee, and H. H. Asada, "A twenty-four hour tele-nursing system using a ring sensor," in *1998 IEEE International Conference on Robotics and Automation*, vol. 1. IEEE, 1998, pp. 387–392.

[10] M.-C. Huang, J. J. Liu, W. Xu, N. Alshurafa, X. Zhang, and M. Sarrafzadeh, "Using pressure map sequences for recognition of on bed rehabilitation exercises," *IEEE Journal of Biomedical and Health Informatics (JBHI)*, vol. 18, no. 2, pp. 411–418, March 2014.

[11] A. Huang, W. Xu, Z. Li, L. Xie, M. Sarrafzadeh, X. Li, and J. Cong, "System light-loading technology for mhealth: manifold-learning-based medical data cleansing and clinical trials in we-care project," *Biomedical and Health Informatics, IEEE Journal of*, vol. 18, no. 5, pp. 1581–1589, 2014.

[12] Q. Wang, G. Xu, and H. Ai, "Learning object intrinsic structure for robust visual tracking," in *2003 IEEE Computer Society Conference on Computer Vision and Pattern Recognition*, vol. 2. IEEE, 2003, pp. II–227.

[13] J. Blackburn and E. Ribeiro, "Human motion recognition using isomap and dynamic time warping," in *Human Motion–Understanding, Modeling, Capture and Animation*. Springer, 2007, pp. 285–298.

[14] M. Zhang, A. Sawchuk *et al.*, "Manifold learning and recognition of human activity using body-area sensors," in *Machine Learning and Applications and Workshops (ICMLA), 2011 10th International Conference on*, vol. 2. IEEE, 2011, pp. 7–13.

[15] A. Valtazanos, D. Arvind, and S. Ramamoorthy, "Using wearable inertial sensors for posture and position tracking in unconstrained environments through learned translation manifolds," in *Proceedings of the 12th international conference on Information processing in sensor networks*. ACM, 2013, pp. 241–252.

[16] W. Xu, M.-C. Huang, N. Amini, J. Liu, L. He, and M. Sarrafzadeh, "Smart insole: A wearable system for gait analysis," in *International Conference on Pervasive Technologies Related to Assistive Environments*, Crete Island, Greece, June 2012, pp. 69 – 72.

[17] F. Lin, X. Xu, A. Wang, L. Cavuoto, and W. Xu, "Automated patient handling activity recognition for at-risk caregivers using an unobtrusive wearable sensor," in *IEEE International Conference on Biomedical and Health Informatics*, February 2016.

[18] Y. Wu, W. Xu, J. J. Liu, M.-C. Huang, S. Luan, and Y. Lee, "An energy-efficient adaptive sensing framework for gait monitoring using smart insole," *IEEE Sensors Journal (SJ)*, vol. 15, no. 4, pp. 2335–2343, April 2015.

[19] F. Lin, A. Wang, C. Song, W. Xu, Z. Li, and Q. Li, "A comparative study of smart insole on real-world step count," in *2015 IEEE Signal Processing in Medicine and Biology Symposium*, Dec 2015, pp. 1–6.

[20] W. Xu, Z. Li, M.-C. Huang, N. Amini, and M. Sarrafzadeh, "ecushion: An etextile device for sitting posture monitoring," in *Body Sensor Networks (BSN), 2011 International Conference on*, May 2011, pp. 194–199.

[21] M. Rofouei, W. Xu, and M. Sarrafzadeh, "Computing with uncertainty in a smart textile surface for object recognition," in *IEEE Conference on Multisensor Fusion and Integration for Intelligent Systems (MFI)*, Salt Lake City, Utah, USA, September 2010, pp. 174 – 179.

[22] A. Nelson and A. Baptiste, "Evidence-based practices for safe patient handling and movement," *Online Journal of Issues in Nursing*, vol. 9, no. 3, p. 4, 2004.

[23] S. Freitag, R. Ellegast, M. Dulon, and A. Nienhaus, "Quantitative measurement of stressful trunk postures in nursing professions," *Annals of Occupational Hygiene*, vol. 51, no. 4, pp. 385–395, 2007.

[24] L. K. Saul and S. T. Roweis, "Think globally, fit locally: unsupervised learning of low dimensional manifolds," *The Journal of Machine Learning Research*, vol. 4, pp. 119–155, 2003.

[25] L. K. Saul, K. Q. Weinberger, J. H. Ham, F. Sha, and D. D. Lee, "Spectral methods for dimensionality reduction," *Semisupervised learning*, pp. 293–308, 2006.

[26] L. K. Saul and S. T. Roweis, "An introduction to locally linear embedding," *unpublished. Available at: http://www. cs. toronto. edu/˜ roweis/lle/publications. html*, 2000.

[27] L. Wang and D. Suter, "Analyzing human movements from silhouettes using manifold learning," in *Video and Signal Based Surveillance, 2006. AVSS'06. IEEE International Conference on*. IEEE, 2006, pp. 7–7.

[28] N. Krause, R. Rugulies, D. R. Ragland, and S. L. Syme, "Physical workload, ergonomic problems, and incidence of low back injury: A 7.5-year prospective study of san francisco transit operators," *American journal of industrial medicine*, vol. 46, no. 6, pp. 570–585, 2004.

[29] I. Jolliffe, *Principal component analysis*. Wiley Online Library, 2002.

[30] C.-H. Joh, T. Arentze, and H. Timmermans, "Pattern recognition in complex activity travel patterns: comparison of euclidean distance, signal-processing theoretical, and multidimensional sequence alignment methods," *Transportation Research Record: Journal of the Transportation Research Board*, no. 1752, pp. 16–22, 2001.

[31] X. Xu, F. Lin, A. Wang, C. Song, Y. Hu, and W. Xu, "On-bed sleep posture recognition based on body-earth movers distance," in *IEEE Conference on Circuits and Systems (BioCAS)*, Atlanta, GA, October 2015, pp. 1 – 4.

[32] H. Ding and J. Xu, "FPTAS for Minimizing Earth Movers Distance under Rigid Transformations and Related Problems," in *21st Annual European Symposium on Algorithms*, 2013.

[33] Z. Hu and L. J. Hong, "Kullback-leibler divergence constrained distributionally robust optimization," *Available on optimization online*, 2012.